Journal of The Electrochemical Society, **156** (12) A1005-A1010 (2009)
0013-4651/2009/156(12)/A1005/6/$25.00 © The Electrochemical Society

Role of AlF_3 Coating on $LiCoO_2$ Particles during Cycling to Cutoff Voltage above 4.5 V

Yang-Kook Sun,[a,*,z] Chong Seung Yoon,[b] Seoung-Taek Myung,[c,*] Ilias Belharouak,[d,*] and Khalil Amine[d,*]

[a]*Department of Energy Engineering and* [b]*Division of Materials Science and Engineering, Hanyang University, Seoul 133-791, South Korea*
[c]*Department of Chemical Engineering, Iwate University, Iwate 020-8551, Japan*
[d]*Electrochemical Technology Program, Chemical Sciences and Engineering Division, Argonne National Laboratory, Argonne, Illinois 60439, USA*

Cell tests demonstrated that the use of an AlF_3 coating enabled a $LiCoO_2$ electrode to deliver a higher discharge capacity (208 mAh g^{-1}) at an upper cutoff voltage of 4.54 V. About 94% of the initial capacity was retained after 50 cycles, while the capacity retention of pristine $LiCoO_2$ was only 60% at 4.5 V. The improved electrochemical performance with the AlF_3 coating was attributed to the delay of structural degradation of $LiCoO_2$ during cycling. A structural analysis of the cycled $LiCoO_2$ electrode revealed that the pristine $LiCoO_2$ transforms to a cubic spinel phase via an intermediate phase triggered by progressive chemical leaching of Co during cycling. The AlF_3 coating protected $LiCoO_2$ from the chemical attack by HF and thus helped to delay the eventual phase transformation to a spinel phase. By delaying this transformation, the AlF_3 coating was able to reduce the charge-transfer resistance and maintain the structural stability when cycled above 4.5 V.
© 2009 The Electrochemical Society. [DOI: 10.1149/1.3236501] All rights reserved.

Manuscript submitted July 9, 2009; revised manuscript received August 27, 2009. Published October 9, 2009.

In recent decades, the demand for small, high capacity batteries to power portable equipment, such as cellular phones and notebook computers, has dramatically risen. Because lithium-ion batteries offer high energy and power density, they have become the most widely used power sources for portable electronic devices and, more recently, hybrid electric vehicles (HEVs) and plug-in HEVs.[1] The most common cathode material for commercial lithium-ion batteries is $LiCoO_2$ due to its high tap density, excellent cycling performance, and high rate capability. Though $LiCoO_2$ has a high theoretical capacity of 274 mAh g^{-1}, its reversible capacity is limited to only 140 mAh g^{-1} when cycled between 3.0 and 4.2 V vs Li metal.

To increase the reversible capacity of $LiCoO_2$, an upper cutoff voltage above 4.2 V should be applied to extract lithium ions beyond $Li_{0.5}CoO_2$. However, as expected, this elevated charge voltage leads to severe capacity loss. Some research groups have reported that the poor cycling performance above 4.2 V is caused by structural instability induced by a phase transition from the hexagonal phase to a monoclinic phase, accompanying a volume change of ~2.6% along the *c*-axis.[2-4] To overcome the above problems, many researchers have modified the $LiCoO_2$ cathode particle surface with metal oxide[5-7] and metal fluoride[8,9] to reduce the catalytic activity of the Co ions with a high oxidation state. Cho et al. reported that ZrO_2-coated $LiCoO_2$, the so-called zero-strain material, delivered a capacity of 170 mAh g^{-1} with an excellent capacity retention after 70 cycles in the voltage range between 2.75 and 4.4 V.[6] Chen and Dahn reported that the capacity loss of $LiCoO_2$ below 4.5 V is mainly due to the interfacial impedance growth between the cathode and electrolyte, which results from side reactions involving $LiPF_6$-based electrolyte and surface impurities caused by air or moisture exposure.[10,11] Recently, Sun et al. also reported that the poor capacity retention of $LiCoO_2$ cycled to 4.5 V stemmed from the increase in charge-transfer resistance and in Co dissolution caused by an HF attack on the cathode surface.[8] More recently, Xia et al. reported that a $LiCoO_2$ thin film (300 nm) shows good capacity retention up to a cutoff voltage of 4.5 V, as no phase transition occurred in the voltage range between 4.2 and 4.5 V.[12]

Structural phase transition and dissolution of a highly oxidized Co^{4+} are responsible for the capacity loss of $LiCoO_2$ above 4.5 V.[13] Van der Ven and Ceder calculated the phase diagram of Li_xCoO_2 ($x < 0.5$) and correlated the phase transition from the O3 phase to the H1-3 phase at around 4.55 V (a stage 2 compound) and from the H1-3 phase to the O1 phase at around 4.62 V.[3] Yazami et al. reported that an aged $LiCoO_2$ electrode charged to 4.7 V underwent the irreversible phase change from a hexagonal to a cubic spinel phase, and the crystals that experienced this phase transformation showed an increased dislocation density and internal strains.[14] Until now, the reason for the enhanced electrochemical performance of the metal-oxide- and metal-fluoride-coated $LiCoO_2$ cathode materials with above 4.5 V cutoff voltage has not been investigated through a detailed structural analysis of the coated cathode during extended cycling.

In this study, we report the excellent capacity exhibited by AlF_3-coated $LiCoO_2$ in the voltage range between 4.5 and 4.6 V and the relation between crystal structure and electrochemical performance at a high cutoff voltage. A pristine $LiCoO_2$ was also tested and characterized at 4.5 V to confirm the capacity fading mechanism.

Experimental

To prepare AlF_3-coated $LiCoO_2$, 0.1 g ammonium fluoride (Aldrich) and 3.91 g aluminum nitrate nonahydrate (Aldrich) were separately dissolved in distilled water. After 50 g $LiCoO_2$ (Nippon Chemical Co.) powders were immersed in the aluminum nitrate nonahydrate solution, the ammonium fluoride solution was slowly added to the resulting solution. The amount of AlF_3 in the solution was 2 mol % of the $LiCoO_2$ powders. After the solution containing the cathode powders was constantly stirred at 80°C for 5 h, it was filtered by distilled water. The obtained $LiCoO_2$ powders were heated at 400°C for 5 h in flowing nitrogen to avoid the formation of Al_2O_3. Details of the coating method are provided in our previous paper.[8,9]

The electrochemical properties of the prepared powder were evaluated with coin-type half-cells (CR2032). Cells were constructed with the electrodes separated by a porous polypropylene film. The electrolyte was a 1:1 mixture of ethylene carbonate (EC) and diethyl carbonate (DEC) containing 1 M $LiPF_6$ by volume (Ukseung Chemical Co., Ltd., Korea). The cathode was fabricated with a mixture of 84 wt % of the prepared powder, 8 wt % carbon black, and 8 wt % poly(vinylidene difluoride) binder on an aluminum current collector. The anode was lithium metal. The cell assembly was carried out in an argon-filled glove box. The capacity and the capacity retention were measured by applying constant currents of 32 mA g^{-1} (0.2 C rate) and 80 mA g^{-1} (0.5 C rate), respectively, between 3.0 and 4.5–4.6 V vs Li/Li^+.

* Electrochemical Society Active Member.
z E-mail: yksun@hanyang.ac.kr

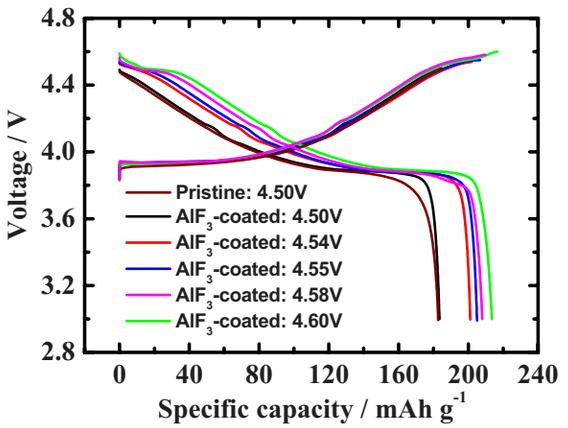

Figure 1. (Color online) Initial charge–discharge curves of Li/pristine $LiCoO_2$ with cutoff voltage of 4.5 V and AlF_3-coated $LiCoO_2$ with cutoff voltages of 4.5–4.6 V at a current density of 32 mA g^{-1} (0.2 C rate).

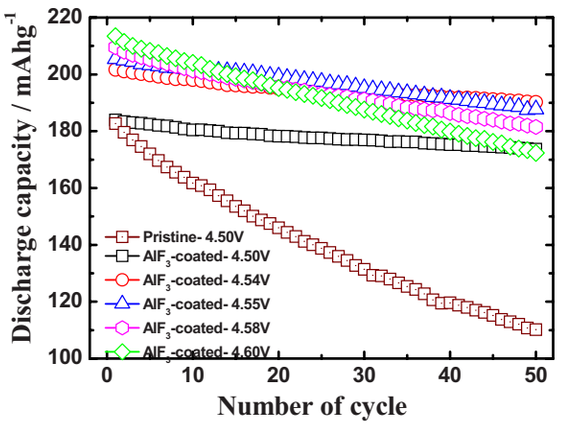

Figure 2. (Color online) Cycling performance of Li/pristine $LiCoO_2$ with cutoff voltage of 4.5 V and AlF_3-coated $LiCoO_2$ with cutoff voltages of 4.5–4.6 V at a current density of 80 mA g^{-1} (0.5 C rate).

AC impedance measurements were performed using a Zahner Elektrik IM6 impedance analyzer over the frequency range of 1 MHz–5 mHz with an amplitude of 10 mV_{rms}. The experiment was carried out for the AlF_3-coated $LiCoO_2$ in a charged state of above 4.5 V as a function of cycle number. To measure the dissolved amount of Co, the coin-type half-cells containing pristine $LiCoO_2$ charged to 4.5 V and AlF_3-coated $LiCoO_2$ charged to an upper cutoff voltage of above 4.5 V were carefully disassembled in a glove box. The recovered cathode active materials were stored in electrolyte at 55°C, and the amount of Co dissolution into electrolyte with storage time was measured by atomic absorption spectroscopy (AAS) (Analytik Jena AG, Vario 6). Transmission electron microscopy (TEM) (JEOL 2010) was employed to observe the phase evolution of the AlF_3-coated Li_xCoO_2 with an upper cutoff voltage above 4.5 V.

Results and Discussion

Figure 1 shows the initial charge/discharge curves of the Li/AlF_3-coated $LiCoO_2$ cells that were obtained by applying a constant current of 32 mA g^{-1} (0.2 C rate) and cutoff voltages between 3.0 and 4.5–4.6 V vs Li/Li^+. For comparison, Fig. 1 shows the initial charge/discharge curve of the Li/pristine $LiCoO_2$ cell charged to 4.5 V. All cells had stable and smooth charge/discharge curves, even above 4.5 V. The discharge capacity of the AlF_3-coated $LiCoO_2$ increased with increasing upper cutoff voltage. The discharge capacity increased by 35% from 4.2 V (140 mAh g^{-1}) to 4.5 V (189 mAh/g) and by 19% from 4.5 to 4.6 V (225 mAh g^{-1}). Also, the AlF_3-coated $LiCoO_2$ delivered a capacity of 208 mAh g^{-1} at a cutoff voltage of 4.54 V. The AlF_3-coated $LiCoO_2$ also had a higher discharge curve than that of the pristine one (cutoff voltage of 4.5 V), especially at the end of discharge, indicating a reduction in the cathode/electrolyte interface resistance, which leads to an increase in energy density of the cell in terms of Wh.[9]

Figure 2 shows the discharge capacity vs cycle number of the Li/AlF_3-coated $LiCoO_2$ cells with various cutoff voltages and the Li/pristine $LiCoO_2$ cell at a 4.5 V cutoff voltage, with a constant current of 80 mA g^{-1} (0.5 C rate). The capacity retention of the AlF_3-coated $LiCoO_2$ decreased as the upper cutoff voltage was raised, especially at 4.6 V. The capacity retention values of the cells at 4.55, 4.58, and 4.6 V after 50 cycles were 91.4, 86.6, and 80.8%, respectively. The capacity retention of the cell with a cutoff voltage of 4.54 V reached 94.3%, which is similar to the 94.4% at 4.5 V. The capacity retention of 94.3% for the cell charged to 4.54 V after 50 cycles is higher than that of 91.4% for the cell charged to 4.55 V even though the charging voltage difference is only 0.01 V. As expected, the pristine $LiCoO_2$ charged to 4.5 V suffers from a severe capacity loss, having a capacity retention of only 61% after 50 cycles.

Figure 3 shows the differential capacity ($dQ\ dV^{-1}$) vs the cell voltage of pristine $LiCoO_2$ and AlF_3-coated $LiCoO_2$ as a function of upper cutoff voltage at the 1st, 10th, 25th, and 50th cycles. The AlF_3-coated $LiCoO_2$ cell exhibited a sharp oxidation peak at 3.94 V. Two minor peaks appeared at 4.08 and 4.20 V during charging due to the multiphase transitions (Fig. 3a). The corresponding reduction peaks are present at 3.88, 4.05, and 4.16 V. The major 3.94 V peak corresponds to the phase transition between the two O3 phases, and two minor peaks correspond to the order–disorder transitions.[2-4] These variations in redox peaks were negligible for the AlF_3-coated $LiCoO_2$ with an upper cutoff voltage of 4.5 and 4.54 V during extensive cycling. No peaks were observed between 4.2 and 4.5 V, suggesting no phase transition in this voltage region and the Li_xCoO_2 still being O3 phase.[12] This result suggests that the AlF_3 coating on the cathode particle does not contribute to the suppression of structural change induced by the phase transition and is quite different from the report on zero-strain materials by Cho et al.[6] In contrast, for the pristine $LiCoO_2$ cycled at 4.5 V, the redox peaks were more polarized and became broader with cycling.[11]

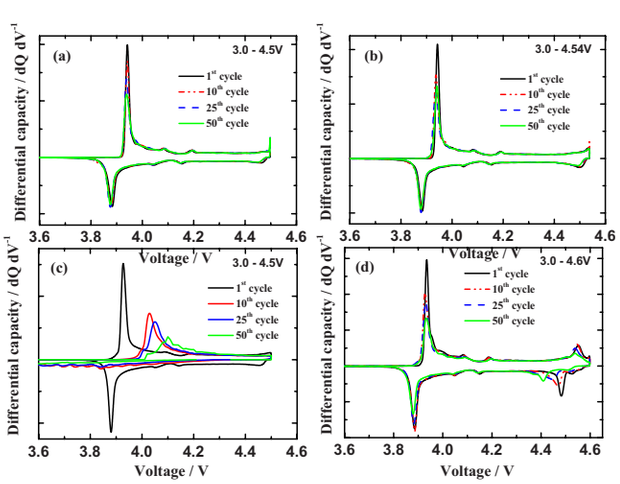

Figure 3. (Color online) Differential capacity vs voltage curves of Li/AlF_3-coated $LiCoO_2$ cells with cutoff voltages of (a) 4.5 and (b) 4.54 V, (c) pristine $LiCoO_2$ with cutoff voltage of 4.5 V, and (d) AlF_3-coated $LiCoO_2$ with cutoff voltage of 4.6 V. Current density of 80 mA g^{-1} (0.5 C rate).

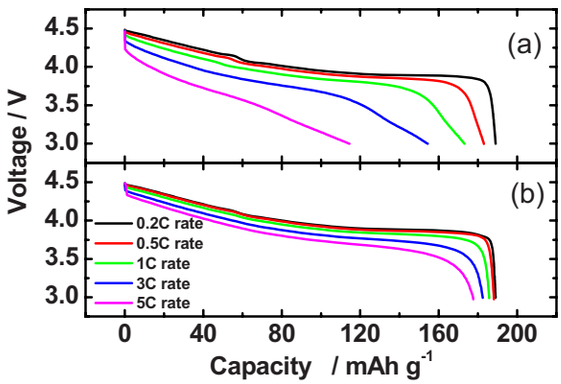

Figure 4. (Color online) Charge/discharge curves of the (a) pristine $LiCoO_2$ and (b) AlF_3-coated $LiCoO_2$ as a function of C rates.

When the upper cutoff voltage was increased to 4.6 V for the AlF_3-coated $LiCoO_2$ (Fig. 3d), a new peak appeared at 4.55 V, which corresponds to the phase transition from the O3 phase to H1-3 phase.[11,12,15] In addition, the redox peaks at 4.55 and 4.48 V changed to a more polarized state, became smaller, and shifted farther apart as the electrochemical cycling proceeded. It is believed that this phase transition from O3 to H1-3 phase is responsible for the capacity fading above an upper cutoff voltage of 4.55 V. Recently, Xia et al. reported that the capacity retention of their $LiCoO_2$ film cell is excellent at an upper cutoff voltage below 4.4 V, degrades slightly when cycled to 4.5 V, and significantly deteriorates above 4.5 V, in which the capacity fade is caused by the structural phase transitions to H1-3 regardless of surface chemistry.[12]

Figure 4 shows the discharge capacities of the Li/pristine and AlF_3-coated $LiCoO_2$ cells as a function of C rate between 3.0 and 4.5 V vs Li. The cells were charged galvanostatically with a 0.2 C rate before each discharge testing, and then discharged at different C rates from 0.2 to 5 C rates (32–800 mA g^{-1}). Clearly, the AlF_3-coated $LiCoO_2$ delivered a higher discharge capacity than the pristine $LiCoO_2$, especially at all the tested C rates. Although the pristine $LiCoO_2$ showed an abrupt discharge capacity at higher currents above a 1 C rate, the AlF_3-coated $LiCoO_2$ electrode retained its higher discharge capacity. At a 5 C rate, the obtained discharge capacity of the AlF_3-coated $LiCoO_2$ was about 93.5%, compared to that of a 0.2 C rate, while the pristine electrode showed a capacity retention of only 60.6% at the same C rate. This result clearly shows the AlF_3-coating impact on the electrochemical performance.

To correlate the structural degradation with interfacial impedance at the interface between the cathode and the electrolyte, electrochemical impedance spectroscopy (EIS) was performed in the AlF_3-coated $LiCoO_2$ charged to different upper cutoff voltages as a function of cycle number, as shown in Fig. 5. The Nyquist plots for the electrodes present two semicircles, one in the high-to-medium frequency region and the other in the low frequency region. According to our previous equivalent circuit concerning EIS,[16] the high-to-medium frequency semicircle is attributed to the resistance of the surface film (R_{sf}) covering the cathode particles, and the low frequency one reflects the charge-transfer resistance (R_{ct}) coupled with a double-layer capacitance. The R_{sf} of the AlF_3-coated $LiCoO_2$ electrodes was almost the same, irrespective of the upper cutoff voltage. However, the R_{ct} value increased with an increase in upper cutoff voltage as well as cycle number at each cutoff voltage; the R_{ct} values at the first cycle were 5.9 Ω at a cutoff voltage of 4.5 V, 10.4 Ω at 4.54 V, and 15.9 Ω at 4.58 V. Table I gives the values obtained for R_{ct} as a function of the number of cycles of the AlF_3-coated $LiCoO_2$ electrodes with different cutoff voltages. As shown by the data, the charge-transfer resistance for the electrode charged to 4.58 V rapidly increased with cycling, while that for the electrodes charged to 4.5 and 4.54 V remained nearly constant. Based on Fig. 3

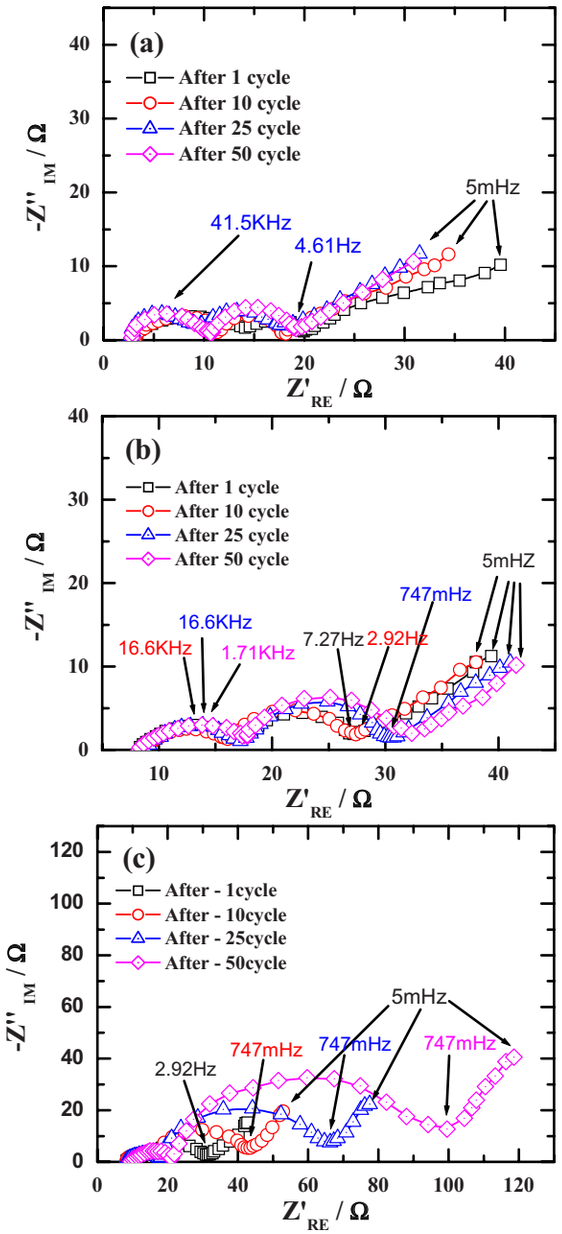

Figure 5. (Color online) Nyquist plots of the Li/AlF_3-coated $LiCoO_2$ with cutoff voltages of (a) 4.5, (b) 4.54, and (c) 4.58 V as a function of cycle number.

and 5, it is speculated that the impedance growth for pristine $LiCoO_2$ cycled at 4.5 V and AlF_3-coated $LiCoO_2$ cycled at 4.58 V

Table I. Charge-transfer resistance (R_{ct}) for AlF_3-coated $LiCoO_2$ cells with different cutoff voltages as a function of cycle number.

	Charge-transfer resistance (Ω)		
Cycle number	4.5 V	4.54 V	4.58 V
1	5.9	10.4	15.9
15	6.8	11.3	26.1
25	8.3	13.5	48.1
50	8.5	14.5	78.4

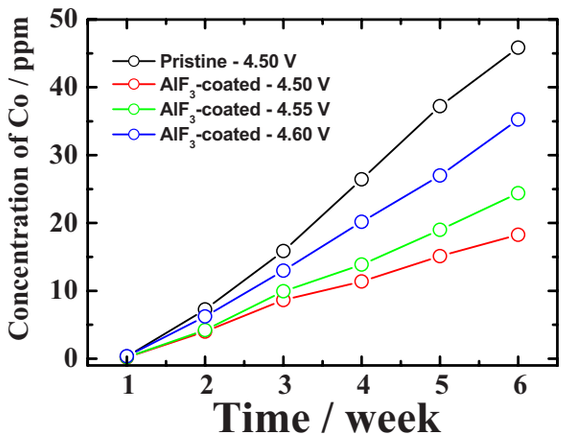

Figure 6. (Color online) Amount of Co dissolution of the pristine and AlF_3-coated $LiCoO_2$ charged to various cutoff voltages as a function of storage time in electrolyte at 55°C.

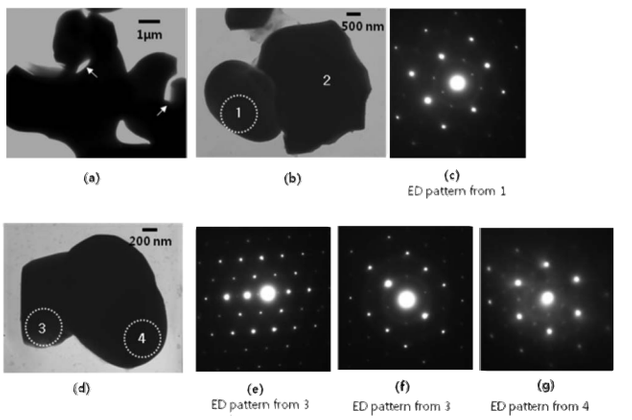

Figure 7. Analytical results of the pristine $LiCoO_2$ after 50 cycles at 4.5 V: (a) TEM image of damaged $LiCoO_2$ particles with arrows showing holes created by a chemical attack during cycling, (b) TEM image of a phase formed on the pre-existing $LiCoO_2$ particle (particle 1 corresponds to this phase, whereas particle 2 is the pre-existing $LiCoO_2$ particle), (c) electron diffraction pattern from particle 1, (d) TEM image showing multiple phases found in the cycled $LiCoO_2$ at 4.5 V, (e) and (f) electron diffraction patterns from particle 3 in two orientations, and (g) electron diffraction pattern from particle 4 indicating a cubic spinel structure (111 zone).

stems from the interface degradation between the cathode and the electrolyte caused by the structural deterioration of the cathode materials.

According to Amatucci et al.,[13] the capacity fading of $LiCoO_2$ cycled between 4.1 and 4.5 V is directly related to cobalt dissolution, which is correlated with large anisotropic structural changes. After testing, the pristine and AlF_3-coated $LiCoO_2$ cathodes were carefully disassembled in a glove box. The recovered cathode materials were stored in their electrolyte [1 M $LiFP_6$ in EC:DEC (1:1 vol %)] at 55°C, and the amount of dissolved Co in the electrolyte solution was measured by AAS. Figure 6 plots the amount of Co dissolution from the pristine and the AlF_3-coated $LiCoO_2$ as a function of storage time. The dissolved amount of Co from the pristine $LiCoO_2$ and AlF_3-coated $LiCoO_2$ increased almost linearly with storage time. However, the Co dissolution from the AlF_3-coated $LiCoO_2$ was substantially suppressed compared with the pristine material, and the amount of Co dissolution was dependent on the upper cutoff voltage, which was consistent with the capacity loss shown in Fig. 2. The Co dissolutions from AlF_3-coated $LiCoO_2$ charged to 4.5, 4.55, and 4.6 V after 6 weeks were 18.3, 24.4, and 35.3 ppm, respectively, which are significantly lower than that for the pristine $LiCoO_2$ charged to 4.5 V (45.5 ppm).

We employed TEM to further analyze the capacity degradation mechanism of the pristine $LiCoO_2$ electrode cycled at 4.5 V. The TEM images of the pristine $LiCoO_2$ particles after 50 cycles revealed that they severely eroded during cycling, which agrees with the Co dissolution data in Fig. 7. A massive Co dissolution from the $LiCoO_2$ electrode can be clearly seen in the TEM bright-field image of the cycled $LiCoO_2$ electrode in Fig. 7a. The particle surface has become rounded, and micrometer-sized voids have formed in the interior of the particles, as indicated by the arrows in Fig. 7a. The image is in striking contrast with those for the as-prepared $LiCoO_2$ electrode before cycling, whose constituent particles are elongated and have straight sides. Figure 7a visually confirms the electrochemical leaching of Co from the electrode when repeatedly cycled at 4.5 V.

In addition to the chemical attack, we observed a phase developing on the surface of the cycled electrode, as shown in Fig. 7b. The particle, labeled 2 in Fig. 7b, has rough edges, indicative of the gradual chemical erosion of a cycled $LiCoO_2$ particle. Particle 1, which appears attached to particle 2, is round and has a smooth surface in contrast to particle 2. The appearance of particle 1 suggests that it nucleated on the pre-existing $LiCoO_2$ particle. The electron diffraction pattern from particle 1, shown in Fig. 7c, could not be indexed to the original $R\bar{3}m$ structure of $LiCoO_2$. The pattern did not match the cubic spinel structure, which was previously observed from the cycled $LiCoO_2$ electrode at 4.7 V.[14] The pattern also did not match either CoO or CoO_2, which are possible phases that can appear during the redox reaction of $LiCoO_2$ with acid.[17] Because this phase could not be detected from X-ray diffraction, the exact crystal structure could not be unambiguously determined. It is believed that a distinctively different phase was formed on the electrode surface during cycling, resulting from a phase transition induced by the progressive Co dissolution. The formation of such a phase is likely responsible for the increased impedance between cathode and electrolyte, thus accelerating the capacity fade of $LiCoO_2$ at 4.5 V. Another example of the coexistence of multiple phases is shown in Fig. 7d. In an attempt to identify particle 3 in Fig. 7d, we conducted electron diffraction of it from two orientations, as shown in Fig. 7e and f; however, neither pattern could be indexed to the original layered structure of $LiCoO_2$ or to the cubic spinel structure. The two patterns appear similar to those of CoO_2 ($P\bar{3}m1$, $a = 2.82$ Å, $c = 4.24$ Å);[18] however, the c/a ratio appears to differ from that of CoO_2 substantially so that the patterns failed to match CoO_2. The electron diffraction pattern from particle 4 matched the 111 zone of a cubic spinel structure. We conjectured that $LiCoO_2$, when cycled at a high cutoff voltage, first transforms to an intermediate phase, yet to be identified, and then to the spinel structure, which is the energetically most stable state for $LiCoO_2$. The phase transformation is most likely triggered by the progressive loss of Co during cycling.

Figure 8 indicates that the AlF_3 coating of the $LiCoO_2$ electrode protects the material from HF attack during cycling. Indeed, a TEM image of the AlF_3-coated $LiCoO_2$ electrode after 50 cycles at 4.5 V in Fig. 8a shows that the particle surface remains intact during cycling, and no severe damage is observed, unlike the pristine counterpart in Fig. 7. Unlike the pristine $LiCoO_2$ electrode, a particle with the original $R\bar{3}m$ structure was rather easily found in the AlF_3-coated $LiCoO_2$ sample. A typical diffraction pattern in the 100 zone of the layered $LiCoO_2$ structure is shown in Fig. 8b. A TEM image of the AlF_3 coating layer remaining after 50 cycles is included in Fig. 8c, which indicates that the AlF_3 coating provides effective protection against the chemical attack from HF in the electrolyte through the electrode's cycle life. Failure to locate the intermediate phase in the AlF_3-coated $LiCoO_2$ sample cycled at 4.5 V suggests that the AlF_3 protection against the Co dissolution also

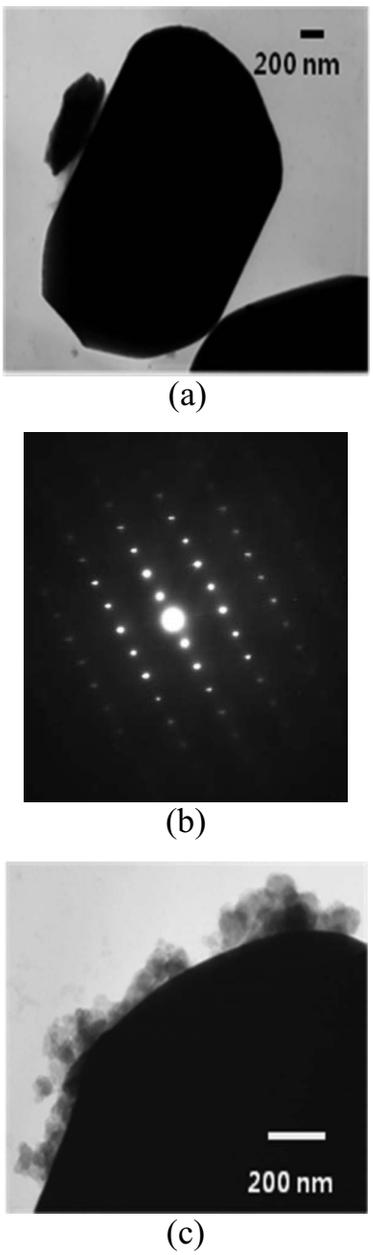

Figure 8. Analytical results of the AlF_3-coated $LiCoO_2$ after 50 cycles at 4.5 V: (a) TEM image showing undamaged particle surface of the AlF_3-coated $LiCoO_2$ electrode, (b) electron diffraction pattern from (a) with the $R\bar{3}m$ structure in 100 zone, and (c) TEM image of AlF_3 coating remaining on the $LiCoO_2$ surface after 50 cycles.

prevented the formation of the secondary phase on the particle surface, blocking the transition to the eventual spinel phase and the accompanying reversible capacity fade.

As the cycling voltage was increased to 4.54 V, the AlF_3-coated $LiCoO_2$ electrode after 50 cycles also started to exhibit formation of an intermediate phase resulting from the Co loss, as shown in Fig. 9. The TEM image in Fig. 9a shows two $LiCoO_2$ particles, which appear to be joined together. It is believed that the particles are in a partially transformed state so that region 1 in Fig. 9a, which appears to be a remnant of the $LiCoO_2$ electrode, retained the original $R\bar{3}m$ structure of $LiCoO_2$, whereas region 2 is the product of the phase transformation. Electron diffraction patterns from each region are

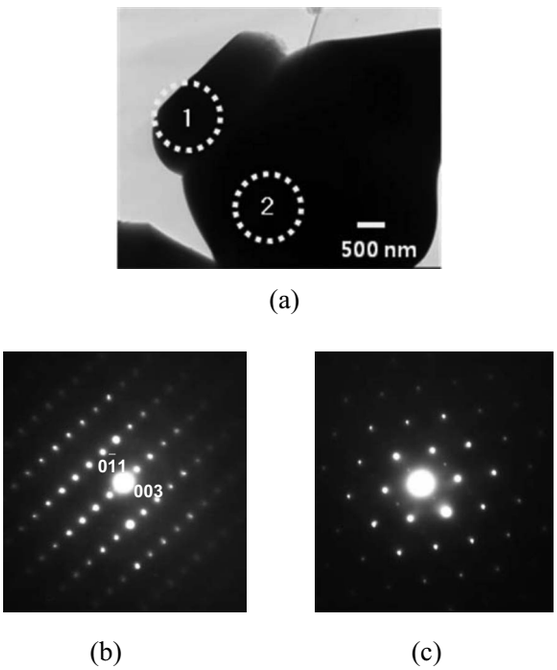

Figure 9. Analytical results from the AlF_3-coated $LiCoO_2$ after 50 cycles at 4.54 V: (a) TEM image of partially transformed $LiCoO_2$ particle, (b) electron diffraction pattern from region 1 in (a), and (c) electron diffraction pattern from region 2 in (a).

presented in Fig. 9b and c. Figure 9b taken from region 1 is unequivocally indexed to the 100 zone of the layered $LiCoO_2$, whereas the diffraction pattern in Fig. 9c cannot be indexed to $R\bar{3}m$ or cubic spinel structures. The interplanar distances estimated from the two diffraction patterns do not coincide, indicating that the two patterns are likely from different crystal structures. As the upper cutoff voltage further increases to 4.55 V, a cubic spinel phase starts to appear in the cycled electrode.

Figure 10a is a TEM image of three distinct regions observed in AlF_3-coated $LiCoO_2$ after 50 cycles at 4.55 V. The electron diffraction patterns in Fig. 10b-d demonstrate that the three regions differ from each other in their crystal structure. Regions 1 and 3 have a cubic spinel phase, and the diffraction patterns are indexed to the 100 and 211 zones of the cubic spinel phase, respectively. Meanwhile, the diffraction pattern from the midregion remains unassigned and is believed to belong to the intermediate phase. In this case, the increased Co dissolution from cycling at 4.55 V induces the increasing conversion of $LiCoO_2$ into the intermediate phase, which was followed by transformation to a spinel phase. At an increased cutoff voltage to 4.58 V, similar to the pristine sample, the AlF_3-coated $LiCoO_2$ was subjected to a severe chemical attack, as can be seen in Fig. 10e. The particle surface is irregular and serrated from extended chemical leaching. The ability of the AlF_3 coating to protect the $LiCoO_2$ electrode from Co dissolution and the accompanying transformations progressively decreases with increasing cutoff voltage.

The TEM analysis of the cycled electrodes shows that when cycled at 4.5 V, the pristine $LiCoO_2$ undergoes a phase transition to a cubic spinel phase via an as-yet unidentified intermediate phase. The transformation is the most likely culprit for the capacity fade observed at 4.5 V by increasing the charge-transfer resistance and thereby decreasing the intrinsic discharge capacity. It is believed that the transformation is triggered by a gradual loss of the Co from the surfaces of the $LiCoO_2$ particles. The AlF_3 coating is effective in protecting $LiCoO_2$ from the dissolution of Co and thus helps to delay the eventual phase transformation to a spinel phase. By delay-

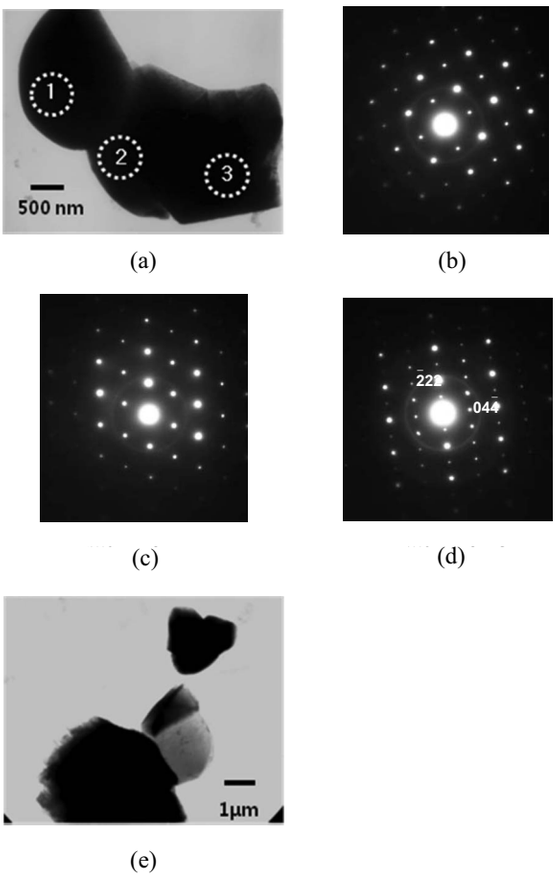

Figure 10. Analytical results from the AlF_3-coated $LiCoO_2$ after 50 cycles at 4.55 and 4.58 V: (a) TEM image of transformed $LiCoO_2$ particle at 4.55 V, [(b), (c), and (d)] electron diffraction patterns from regions 1, 2, and 3, respectively, and (e) TEM image of damaged $LiCoO_2$ particles at 4.58 V.

ing the transformation, the AlF_3 coating allows the $LiCoO_2$ electrode to maintain the reversible capacity above 4.5 V.

Conclusions

The effect of an AlF_3 coating on $LiCoO_2$ electrodes cycled at cutoff voltages above 4.5 V was investigated. The AlF_3 coating enabled the $LiCoO_2$ electrode to achieve a capacity retention greater than 90% after 50 cycles, even at a 4.55 V cutoff, while the pristine $LiCoO_2$ exhibited a capacity retention of only 60% at 4.5 V. The improved electrochemical performance with the AlF_3 coating was attributed to the lowered charge-transfer resistance caused by the delay of the structural degradation of the electrode. The Co dissolution data, together with the TEM analysis, explicitly demonstrated that the AlF_3 coating protects $LiCoO_2$ from the dissolution of Co and thus helps to delay the eventual phase transformation to a spinel phase during cycling. By delaying the transformation, the AlF_3 coating reduces the charge-transfer resistance and allows the electrode to maintain its structural stability when cycled above 4.5 V.

Acknowledgments

This work was supported by the Global Research Network Program and by a World Class University (WCU) program through the Korea Science and Engineering Foundation by Education, Science, and Technology (R31-2008-000-10092).

Hanyang University assisted in meeting the publication costs of this article.

References

1. K. Amine, C. H. Chen, J. Liu, M. Hammond, A. Jansen, D. Dees, I. Bloom, D. Vissers, and G. Henriksen, *J. Power Sources*, **97–98**, 684 (2001).
2. J. N. Reimers and J. R. Dahn, *J. Electrochem. Soc.*, **139**, 2091 (1992).
3. A. Van der Ven, M. K. Aydinol, G. Ceder, G. Kresse, and J. Hafner, *Phys. Rev. B*, **58**, 2975 (1998).
4. T. Ohzuku and A. Ueda, *J. Electrochem. Soc.*, **141**, 2972 (1994).
5. H.-J. Kweon, G.-B. Kim, and D.-G. Park, K.R. Pat. 0,420,034 (2004).
6. J. Cho, Y. J. Kim, T. J. Kim, and B. Park, *Angew. Chem., Int. Ed.*, **40**, 3367 (2001).
7. Y.-K. Sun, Y.-S. Lee, M. Yoshio, and K. Amine, *Electrochem. Solid-State Lett.*, **5**, A99 (2002).
8. Y.-K. Sun, J.-M. Han, S.-T. Myung, S.-W. Lee, and K. Amine, *Electrochem. Commun.*, **8**, 821 (2006).
9. Y.-K. Sun, S.-W. Cho, S.-T. Myung, K. Amine, and J. Prakash, *Electrochim. Acta*, **53**, 1013 (2007).
10. Z. H. Chen and J. R. Dahn, *Electrochem. Solid-State Lett.*, **6**, A221 (2003).
11. Z. H. Chen and J. R. Dahn, *Electrochim. Acta*, **49**, 1079 (2004).
12. H. Xia, L. Lu, Y. S. Meng, and G. Ceder, *J. Electrochem. Soc.*, **154**, A337 (2007).
13. G. G. Amatucci, J. M. Tarascon, and L. C. Klein, *Solid State Ionics*, **83**, 167 (1996).
14. R. Yazami, Y. Ozawa, H. Gabrisch, and B. Fultz, *Electrochim. Acta*, **50**, 385 (2004).
15. Z. Chen, Z. Lu, and J. R. Dahn, *J. Electrochem. Soc.*, **149**, A1604 (2002).
16. Y.-K. Sun, S.-T. Myung, C. S. Yoon, and D.-W. Kim, *Electrochem. Solid-State Lett.*, **12**, A163 (2009).
17. R. J. Gummow, M. M. Thackeray, W. I. F. David, and S. Hull, *Mater. Res. Bull.*, **27**, 327 (1992).
18. T. Motohashi, T. Ono, Y. Katsumata, R. Kanno, M. Karppinen, and H. Yamauchi, *J. Appl. Phys.*, **103**, 07C902 (2008).